Drug Development and Industrial Pharmacy, 22(9&10), 933–942 (1996)

Influence of Punch Velocity on the Compressibility of Granules

Kazumi Danjo,* Hideo Kimura, and Akinobu Otsuka

Faculty of Pharmacy, Meijo University, 150 Yagotoyama, Tempaku-ku, Nagoya 468, Japan

ABSTRACT

The influence of punch velocity over the range 1–30 mm/min on the compressibility of granules and particles was studied using a modified Kawakita equation. Granule strength (S_t) increased with increasing concentration and viscosity of binder solution as well as increasing mean molecular weight of binding agent. The compressibility of powders was evaluated by the modified Kawakita equation (K). For the granules, the relationship between pressure and reciprocal of porosity ($1/\varepsilon$) showed an inflection point, but for the particles, no such inflection point was found. The slope of low compression stress in the stage of densification by powder slippage and rearrangement was the constant K_1; and slope of high compression stress in the stage of elastic, plastic deformation and plastic fracture of particles was the constant K_2. The K_1 values decreased with increasing punch velocity. An approximately linear relationship was observed between reciprocal of compressibility constant ($1/K_2$) and granule strength (S_t). For crystalline lactose, K values decreased with increasing punch velocity, indicating that compressibility was lowered. Thus, compressibility was shown to be dependent on type of crystal. The quantity of stress relaxation increased with increasing punch velocity. Especially, constant a and b values in a cellulose system (HPC) were greater than those in a noncellulose system (PVP). As a good relationship was found between constants a, b and constant K_2, materials which undergo plastic deformation and fragmentation have great stress relaxation. The radial tensile strength (σ_t) increased with increasing granule strength (S_t). We concluded from these findings that the σ_t value was affected by the contact area rather by than the number of contact points.

*To whom correspondence should be addressed.

INTRODUCTION

There are many factors which affect the compressibility of particles, such as particle size, shape, distribution, and surface conditions; and also punch velocity, surface condition of punch and die, and surrounding conditions in tablet machines. Rowe and Roberts (1) investigated the effects of punch velocity on the yield pressure using the Heckel equation. Newton and Pitt (2) studied the relationship between punch velocity and tablet strength, and reported that tablet strength decreased with increasing punch velocity. Seitz and Flessland (3) and Fell and Newton (4) have reported that the apparent density of tablets increased with decreasing punch velocity for particles with a high degree of plasticity, but that of fragile particles was not affected by punch velocity. David and Augsburger (5) and Armstrong (6) concluded that tablet strength was easily affected by punch velocity for plastic particles. On the other hand, York et al. (7) investigated the relationship between punch velocity and capping phenomena. However, these experiments did not address the effects exerted by the punch velocity on the compressibility or stress relaxation using the same powder and/or granules.

This study was carried out to investigate the effects of punch velocity on the compressibility and stress relaxation of the same powders and granules.

EXPERIMENTAL

Materials and Methods

Materials The sample powders used were α-lactose monohydrate (DMV 200), β-lactose anhydrate (Taiyo Chemical Co., Ltd.) and tablettose (Meggle 80). Granules were prepared using α-lactose monohydrate and polyvinylpyrrolidone (BASF, PVP K30, K90) and hydroxypropylcellulose (Shin Etsu EF-P, LF-P) as binders. Table 1 shows the physicochemical properties of the binder solutions and granule diameters.

Measurement of Viscosity Binder solution viscosity was measured at 20°C with an E-type viscometer (Tokyo Keiki Co., Ltd.).

Granulation Method Granulation experiments were conducted with an agitating–fluidized bed granulator (Powrex Co., Ltd., type MP-01). Five hundred grams of α-lactose monohydrate was preagitated at 350 rpm, and 130 g of binder solution was then sprayed onto the lactose. The following granulating conditions were kept constant for all batches: inlet air temperature, 75°C; outlet air temperature, 35°C; and fluid flow rate, 12 g/min 100 g of binder solution. Soon after, 130 g of binder solution was sprayed at 15 sec of intermittance.

Measurement of Granule Diameter Distribution Granule diameter distribution was determined with JIS standard sieves vibrated on a sieve-shaking machine. The mean granule diameter (D_{50}) is equivalent to the median diameter.

Measurement of Granule Hardness Granule hardness was measured with a hardness tester, as described previously (8). The values shown represent the means and standard deviations of 30 granules. The granule strength, S_t, was obtained by the Hiramatsu equation (9):

$$S_t = 2.8W/(\pi d^2) \quad (1)$$

Table 1

Physicochemical Properties of Binder Solution and Mean Granule Diameter (D_{50})

Binder Solution	Mean Molecular Weight, M_w[a]	Viscosity[b] (mPa·s)	D_{50} (μm)
5% HPC EF-P	56,000	33.36	246.44
7% HPC EF-P	56,000	93.24	257.11
5% HPC LF-P	93,000	186.48	290.89
7% HPC LF-P	93,000	484.20	322.40
5% PVP K-30	45,000	4.38	155.88
7% PVP K-30	45,000	36.06	189.48
5% PVP K-90	1100,000	84.00	371.28
7% PVP K-90	1100,000	352.20	409.53

[a]Manufacturer's data
[b]Measured at 20°C

where W is the maximum load at the fracture of the granule and d is the granule diameter.

Compression Test and Measurement of Radial Tensile Strength All samples were compressed on a universal tension and compression tester (Shimadzu Autograph AG 5000D) with 16-mm flat-face punches to a tablet weight of 1.0 g. Using the Autograph, we subjected the model tablets to a diametral compression test after they had been allowed to remain at room temperature for 24 h. The test consisted of applying a load diametrically, measuring the maximum load, F, at the tablet fracture, and calculating the radial tensile strength, σ_t, using the following equation:

$$\sigma_t = 2F/(\pi D_t) \quad (2)$$

where D is the tablet diameter and t is the tablet thickness.

Measurement of Stress Relaxation Stress relaxation experiments were performed using an Autograph equipped with 16-mm flat-face punches to a tablet weight of 1.0 g. The evolution of the force in relation to time caused by the upper punch displacement was then recorded during 30 min.

Measurement of Specific Permeability Specific permeability of the compressed tablets in terms of air permeation was measured with a Shimadzu powder surface area determinator (model ss-100).

Measurement of Pore Volume Distribution in the Tablets The pore volume distribution in the tablets was determined using a mercury porosimeter (Shimadzu-Micromeritics Pore sizer 9305).

RESULTS AND DISCUSSION

Effects of Properties of Binder Solution on the Granule Strength

Granule strength increased with increasing binder solution concentration, binder solution viscosity, and molecular weight of binding agent, as shown in Table 2. On the other hand, fracture strength of α-lactose monohydrate particles showed a tendency to be greater than those of β-lactose anhydrate and tablettose. Furthermore, fracture strength of powder particles showed large values, compared with granule strength. It was considered that the fracture strengths of granules and tablettose particles were small due to the presence of pores in the particles, as mentioned later.

Table 2

Particle Strength and Granule Strength

Particles	Particle Strength[a] (10^{-2} kN/m^2)	d_p (μm)
α-Lactose monhydrate	51.04 (± 11.86)	202.7
β-Lactose anhydrous	30.00 (± 8.45)	186.1
Tablettose	3.11 (± 1.13)	166.9
Granules	**Granule Strength[a] (10^{-2} kN/m^2)**	
5% HPC EF-P (EG5)	3.31 (± 1.75)	
7% HPC EF-P (GE7)	3.78 (± 2.28)	
5% HPC LF-P (GL5)	4.30 (± 2.66)	
7% HPC LF-P (GL7)	5.18 (± 2.66)	
5% PVP K-30 (GK35)	2.92 (± 1.41)	
7% PVP K-30 (GK37)	2.94 (± 1.54)	
5% PVP K-90 (GK95)	5.37 (± 2.33)	
7% PVP K-90 (GK97)	9.45 (± 3.90)	

[a]Mean ± SD.

Effects of Punch Velocity on the Compressibility of Granules

The effects of punch velocity on the compressibility of granules and powder particles were examined. We assumed that the relationship between porosity and compression force conformed to the following modified version of the Kawakita equation for the compression process (10):

$$-(d\varepsilon/dP) = K\varepsilon^2 \quad (3)$$

where ε is the porosity of the compaction layer, P is the compression force, and K is a constant which is related to the compressibility of powder and granules. Equation (3) represents the following linear relations:

$$1/\varepsilon = 1/\varepsilon_0 + KP \quad (4)$$

where ε_0 is the initial porosity at $P = 0$.

Porosity (ε) decreased with increasing compression force (P) for the samples of G_{E7}, as shown in Fig. 1. Other samples showed the same tendency as sample G_{E7}. Figure 2 shows the relationship between compression force (P) and reciprocal of porosity (1/ε) for each sample. The results for powder particles showed good linearity, but those for granule samples showed an inflection point at the initial stage of the compression process. Thus, we divided the compression process into two stages. In the first, stage, K_1, particles were consolidated mainly by filling, slippage, rearrangement, and

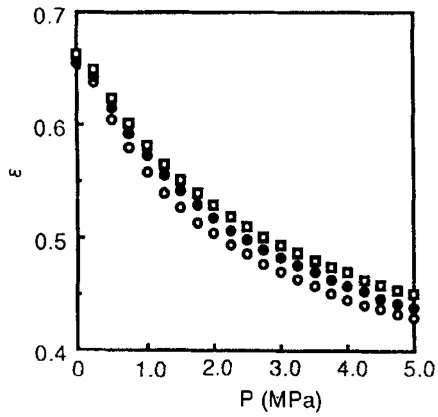

Figure 1. Relationship between compression stress and porosity for G_{E7}. ○, 1 mm/min; ●, 10 mm/min; □, 30 mm/min.

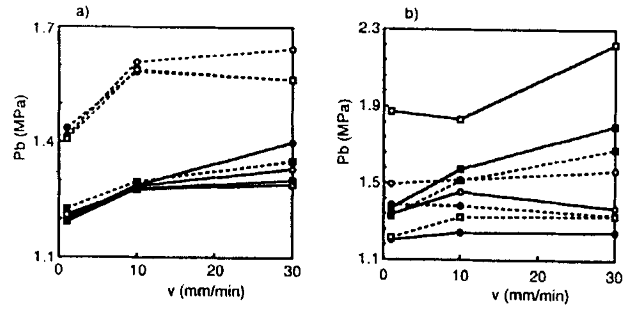

Figure 3. Relationship between punch velocity and inflection point (P_b). (a) Cellulose system; ○, 5% EF-P; ●, 7%, EF-P; □, 5% LF-P; ■, 7% LF-P. (b) PVP system; ○, 5% K-30; ●, 7% K-30; □, 5% K-90; ■, 7% K-90. Dotted lines are 150 μm; solid lines are 210 μm.

elastic deformation of particles; and at the second stage, K_2, consolidation of particles was accompanied by plastic deformation and plastic fracture of particles.

Here we discuss the effects of punch velocity on the constant K_1 and K_2. We considered the inflection point P_b to represent the beginning of plastic fracture of the granules. The values of P_b increased with increasing punch velocity (v) as shown in Fig. 3. P_b value was shifted to high compression stress due to the nonuniform transition of applied pressure in the compacted layer when the punch velocity was high. Generally, the P_b value increased with increasing granule strength, but when using binding agent in the HPC system, the P_b value was independent of granule strength as well as binder solution concentration until 10 mm/min punch velocity, as shown in Fig. 3(a). On the other hand, when using the binding agent of the PVP, the P_b value increased with increasing granule strength at punch velocities over 5 mm/min, as shown in Fig. 3(b). However, the P_b value was independent of punch velocity due to brittleness of granules prepared using PVP-K30 as reported by Fell and Newton (4). Furthermore, P_b values increased with increasing granule diameter in the HPC system. Kato et al. (10) reported the same results using large particles.

Slippage and rearrangement of particles were considered to occur at incipient compaction due to the greater compressibility of particles with a large diameter compared with those of small diameter. In these results, failure process changed to lower compression stress and then P_b value became low. On the other hand, slippage and rearrangement of particles occurred at high compression stress due to the greater adhessiveness of small particles in comparison with large particles.

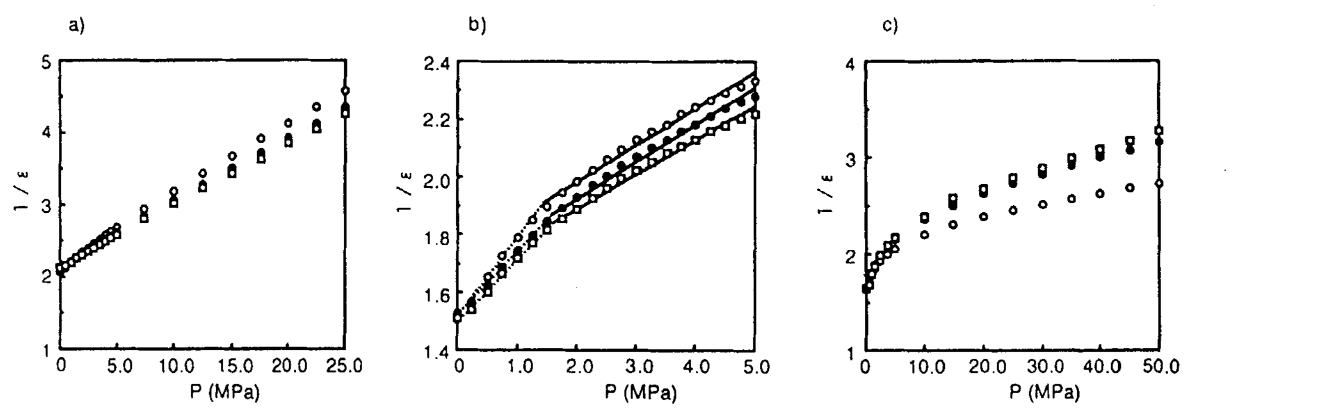

Figure 2. Plots of the modified Kawakita equation as a function of punch velocity: (a) powder particle; (b) granule; (c) tablettose. ○, 1 mm/min; ●, 10 mm/min; □, 30 mm/min.

Next, we examined the effects of punch velocity on the constant K_1. The value of $1/K_1$ increased with increasing punch velocity as shown in Fig. 4. It was suggested that the compressibility during the particle rearrangement decreased with increasing punch velocity due to the decrease in transmittance of compression stress with increasing punch velocity. The PVP system showed larger values of $1/K_1$ compared with those of the HPC system as shown in Figs. 4(a) and 4(b). It was considered that the granules prepared using the PVP system flowed more easily than those of the HPC system due to the greater surface roughness of granules in the former compared with the latter. Furthermore, small-sized particles showed a tendency to have higher values of $1/K_1$ indicating low compressibility due to the greater apparent adhesiveness between particles than in those of larger particle size. On the other hand, for powder particles, the value of $1/K$ increased with increasing punch velocity as observed for $1/K_1$ value of granules. However, $1/K$ as α-lactose monohydrate has smaller particles with smoother surfaces than those of β-lactose anhydrate, α-lactose monohydrate showed increased compressibility due to better transmission of compression stress.

York (11) estimated the value of particle densification (ρ_{FB}) due to particle slippage and rearrangement according to the following equation:

$$\rho_{FB} = F\rho_{FA} - \rho_{FO} \qquad (5)$$

where ρ_{FA} is the densification due to die filling and particle slippage and rearrangement, and ρ_{FO} is the initial powder packing fraction. Figure 5 shows the effects of punch velocity on ρ_{FB}; ρ_{FB} showed a tendency to decrease with increasing punch velocity. Further, ρ_{FB} values of materials with large granule size were greater than those of smaller granules and showed greater values in granules prepared by the PVP system than in those prepared by the HPC system, as shown in Figs. 5(a) and 5(b). These ρ_{FB} values showed the same tendency as the values of K_1. The constant K_1 appered to be useful for determining the initial compressibility due to slippage and rearrangement of granules. ρ_{FB} values of powder particles were compared with those of granules at compression stress of 1.5 MPa; ρ_{FB} values of powder particles were smaller than those of granules, as shown in Fig. 5(c), because the granules show better compressibility than powder particles. However, ρ_{FB} values of α-lactose monohydrate particles were lower than those of β-lactose anhydrate particles due to the greater initial apparent volume of the latter, and the reduction of apparent volume of β-lactose particles increased. On the other hand, tablettose showed good compressibility due to facilitated slippage and rearrangement of granule particles.

Figure 6 shows the relationship between punch velocity and reciprocal of constant K_2 which represent the second stage consolidated by plastic deformation and plastic fracture of particles. $1/K_2$ values tendened to decrease with increasing punch velocity and the compressibility of particles in the second stage increased with increasing punch velocity. These results are in contrast to the general observation that compressibility decreased with increasing punch velocity, but it was considered that plastic deformation accounted for the

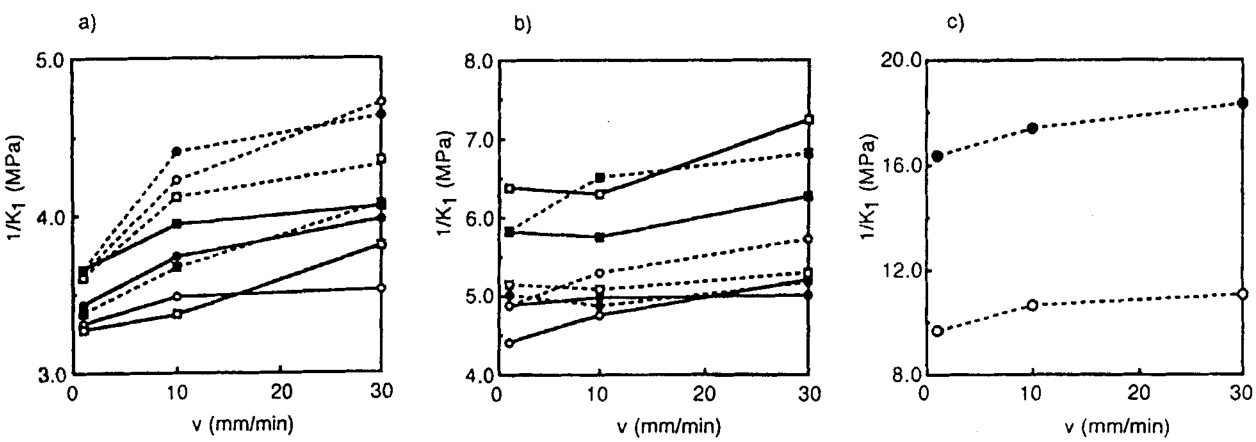

Figure 4. Relationship between punch velocity and reciprocal of constant K_1 and K. (a) Cellulose system; ○, 5% EF-P; ●, 7% EF-P; □, 5% LF-P; ■, 7% LF-P. (b) PVP system; ○, 5% K-30; ●, 7% K-30; □, 5% K-90; ■, 7% K-90. (c) Powder particles; ○, α-lactose monohydrate; ●, β-lactose anhydrate. Dotted lines are 150 μm; solid lines are 210 μm.

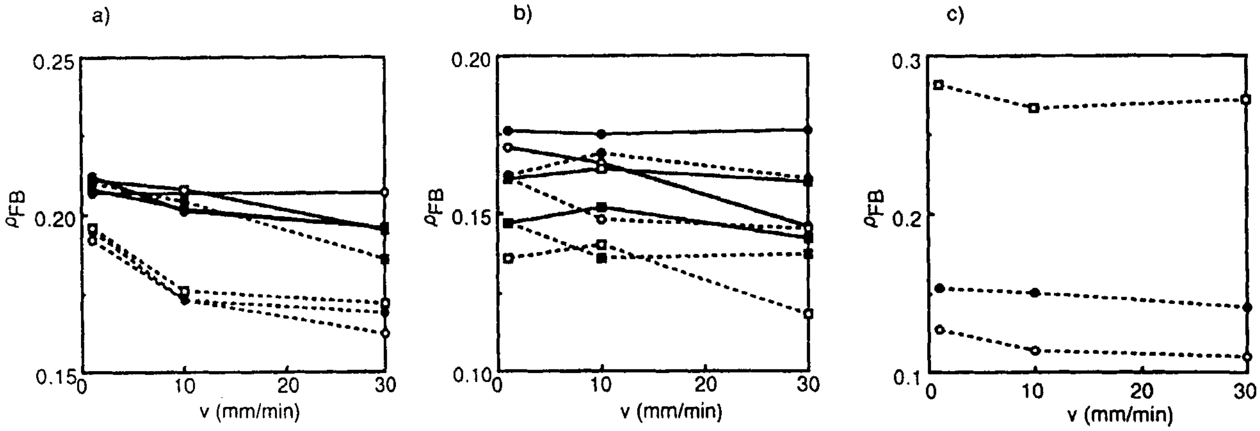

Figure 5. Relationship between punch velocity and value of ρ_{FB}. (a) Cellulose system; ○, 5% EF-P; ●, 7% EF-P; □, 5% LF-P; ■, 7% LF-P. (b) PVP system; ○, 5% K-30; X, 7% K-30; □, 5% K-90; ■, 7% K-90. (c) Powder particles; ○, α-lactose monohydrate; ●, β-lactose anhydrate. Dotted lines are 150 μm; solid lines are 210 μm.

majority of the compression process rather than plastic fracture for granules.

The granule strength (S_t) and reciprocal of constant K_2 showed a good correlation (Fig. 7). These results suggested that the constant K_2 is closely related with plastic deformation and plastic fracture of particles.

Figure 8 shows the relationship between reciprocal of constant K_2 and radial tensile strength, σ_t; σ_t showed a tendency to increase with increasing $1/K_2$ values. Generally, radial tensile strength increased with increasing plastic deformation and plastic fracture of particles, contrary to the general observations. We assume that the radial tensile strength increased with increasing contact area of particles in the tablet due to the predominance of plastic deformation over plastic fracture at high punch velocity.

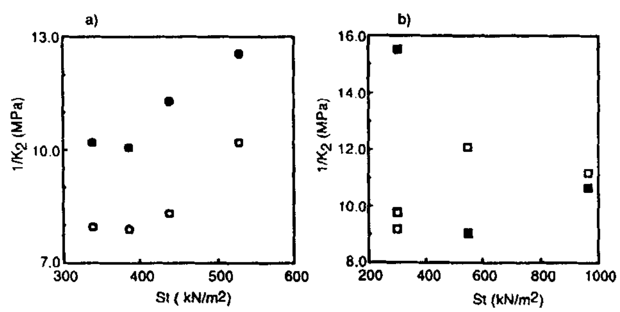

Figure 7. Relationship between granule strength and reciprocal of constant K_2 at punch velocity of 1 mm/min. (a) Particle diameter is 150 μm; ○, HPC; □, PVP. (b) Particle diameter is 210 μm; ●, HPC; ■, PVP.

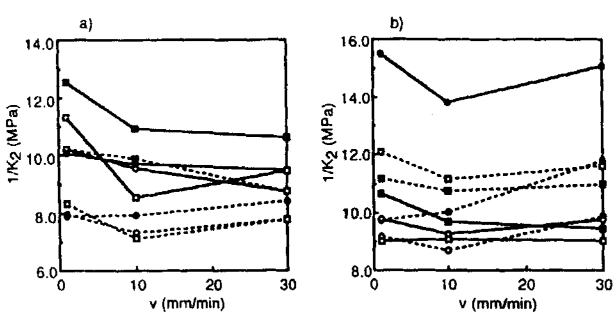

Figure 6. Relationship between punch velocity and reciprocal of constant K_2. (a) Cellulose system; ○, 5% EF-P; ● 7% EF-P; □, 5% LF-P; ■, 7% LF-P. (b) PVP system; ○, 5% K-30; ●, 7% K-30; □, 5% K-90; ■, 7% K-90. Dotted lines are 150 μm; solid lines are 210 μm.

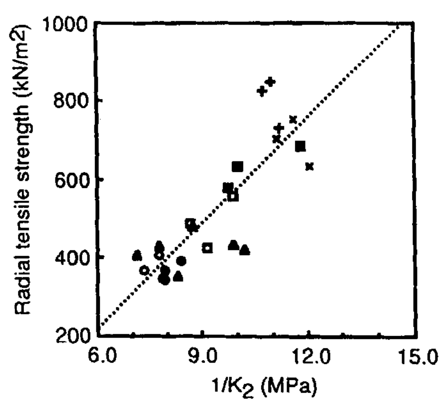

Figure 8. Relationship between reciprocal of constant K_2 and radical tensile strength for 150-μm particle diameter. ○, 5% EF-P; ●, 7% EF-P; Δ, 5% LF-P; ▲, 7% LF-P; □, 5% K-30; ■, 7% K-30; ×, 5% K-90; +, 7% K-90.

To further clarify the reasons behind these phenomena, we examined the effects of granule strength on radial tensile strength, as shown in Fig. 9. Radial tensile strength increased with increasing granule strength for each punch velocity, and thus it was assumed that the radial tensile strength increased due to increases in contact area of particles with large plastic deformation when fracture of granules did not occur easily.

Effects of Punch Velocity on Stress Relaxation

We investigated the effects of punch velocity on stress relaxation using a Shimadzu Autograph universal tension and compression tester. Figure 10 shows the stress relaxation with punch velocities of 1 mm/min, 10 mm/min, and 30 mm/min under constant strain, and it can be seen that the stress relaxation increased with increasing punch velocity for each sample.

Many equations (12–15) have been reported for stress relaxation. Here, however, experimental data were arranged following Peleg's (16) equation:

$$Y(t) = (F_0 - F_t)/F_0 \tag{6}$$

where $F(t)$ is the decaying parameter in terms of force or stress, F_0 is the initial force, and F_t is the decaying force after time t; and fitted to following equation:

$$Y(t) = (abt)/(1 + bt) \tag{7}$$

$$1/Y(t) = 1/(ab) + t/a \tag{8}$$

where a and b are experimental constants. a is the saturated stress; for example, if $a = 1.0$ the stress relates to zero level as in the case of liquids. b represent the steepness of the decay; for example, $1/b$ is the time to reach the level of $a/2$. Figure 11 shows that $Y(t)$ values were almost constant after 60 min.

Figure 12 plots Eq. (8), at relaxation time up to 10 sec for the G_{E5} sample. It can be seen that there is a good relationship for each sample.

The constants a and b were obtained by the slope and intercept from the straight line and plotted against punch velocity as shown in Fig. 13. These findings show that

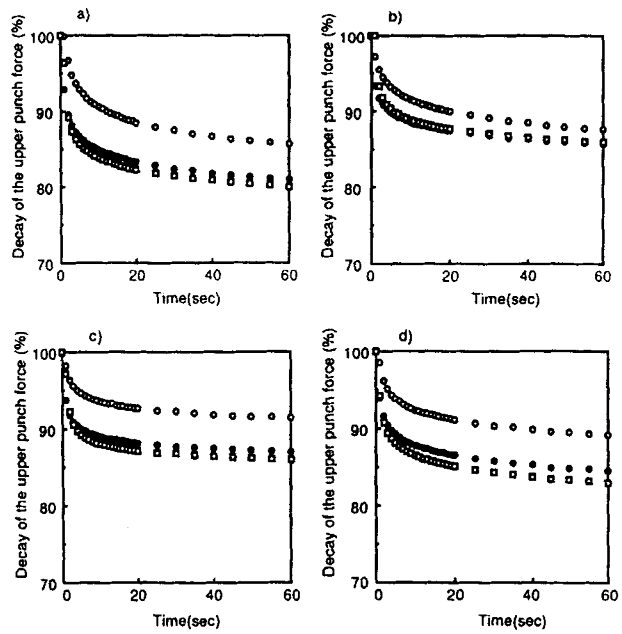

Figure 10. Relaxation stress curves: (a) HPC system; (b) PVP system; (c) α-lactose monohydrate; (d) β-lactose anhydrate. ○, 1 mm/min; ●, 10 mm/min; □, 30 mm/min.

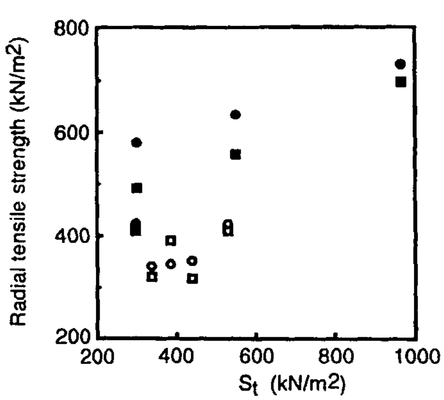

Figure 9. Relationship between granule strength and radial tensile strength for 1 mm/min punch velocity. ○, HPC 150 μm; ●, HPC 210 μm; □, PVP 150 μm; ■, PVP 210μm.

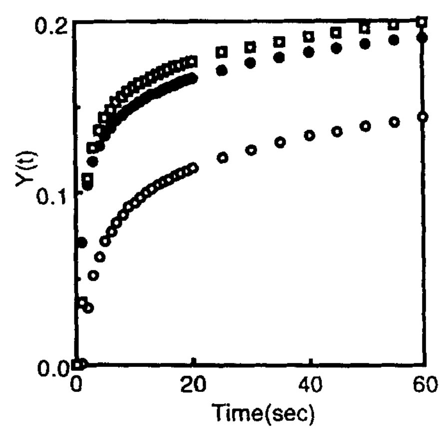

Figure 11. Relationship between stress relaxation time and $Y(t)$ for G_{E5}. ○, 1 mm/min; ●, 10 mm/min; □, 30 mm/min.

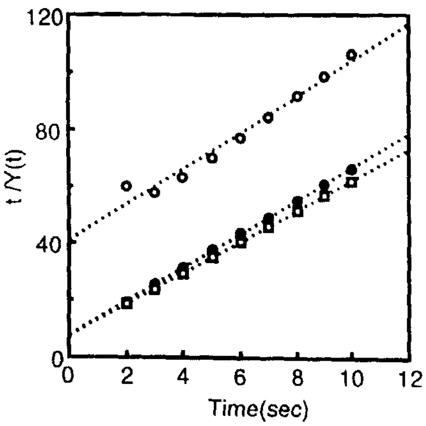

Figure 12. Relationship between stress relaxation time and $t/Y(t)$ for G_{E5}. ○, 1 mm/min; ●, 10 mm/min; □, 30 mm/min.

a and b increased with increasing punch velocity. It was considered that the particles easily moved into pores in the tablet due to force transfer becoming nonuniform with increasing punch velocity. For granules, HPC of cellulose type (dotted line) showed greater stress relaxation than PVP (solid line) as shown in Fig. 13(a). On the other hand, for powder particles, α-lactose monohydrate particles did not undergo stress relaxation to a greater degree than β-lactose anhydrate particles, as shown in Fig. 13(b). This was due to their ease of compaction as described above, because α-lactose monohydrate has higher density and a smoother particle surface than β-lactose anhydrate. Tablettose showed the lower stress relaxation than α- and β-lactose due to its ease of flow and compaction. Further, stress relaxation values of granules were larger than those of powder particles as shown in Figs. 13(a) and 13(b). These findings show that granules easily undergo plastic deformation. As stated above, these properties were reflected in P_b values. On the other hand, large-sized particles underwent stress relaxation more easily than small particles due to the larger pore volume in the tablet.

We investigated the relationship between the compressibility and the stress relaxation. Figure 14 shows the relationship between reciprocal of constant K_2 in relation to compressibility of particles after the inflection point, P_b and constant a and b relate to stress relaxation. These findings show that the values of a and b increased with decreasing values of $1/K_2$, and it was confirmed that plastic deformation and plastic fracture of materials are more easily relaxed.

Next, we investigated the effects of stress relaxation on radial tensile strength, σ_t. Figure 15 shows the relationship between constant a and σ_t; σ_t increased with increasing value of constant a, and σ_t of β-lactose anhydrate was about twice that of α-lactose monohydrate.

Effects of Punch Velocity on the Internal Structure of Tablets

If we assume that the stress relaxation occurs mainly as a result of movement of particles, it will be affected

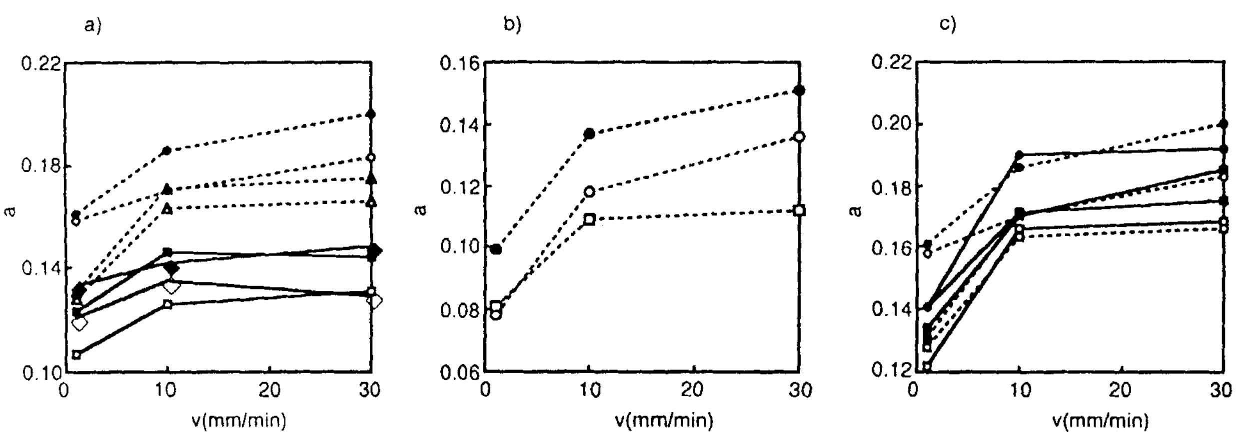

Figure 13. Relationship between punch velocity and constant a. (a)---○---, 5% EF-P 150 μm; ---●---, 7% EF-P 150 μm; ---△---, 5% LF-P 150 μm; ---▲---, 7% LF-P 150 μm; —□—, 5% K-30 150 μm; —■—, 7% K-30 150 μm; —◇—, 5% K-90 150 μm; —◆—, 7% K-90 150 μm. (b) ---○---, α-lactose monohydrate; ---●---, β-lactose anhydrate; ---□---, tablettose, (c) ---○---, 5% EF-P 150 μm; ---●---, 7% EF-P 150 μm; ---□---, 5% LF-P 150 μm; ---■---, 7% LF-P 150 μm; —○—, 5% EF-P 210 μm; —●—, 7% EF-P 210 μm; —□—, 5% LF-P 210 μm; —■—, 7% LF-P 210 μm.

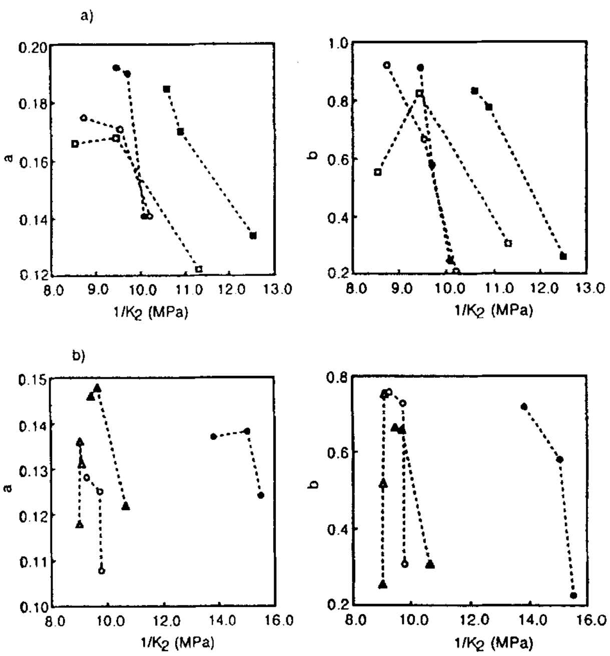

Figure 14. Relationship between reciprocal of constant K_2 and constants *a* and *b*. (a) HPC system; (b) PVP system; ○, 5% EF-P; ●, 7% EF-P; □, 5% LF-P; ■, 7% LF-P.

by pore volume in the tablet. To clarify this we performed the following experiments. Figure 16 shows the effects of punch velocity (v) on the specific permeability (P_a) of α-lactose monohydrate and β-lactose anhydrate tablets; the values of P_a increased with increasing punch velocity. These results suggested that the particles moved easily into the pores at high punch velocity, supporting the observation that stress relaxation increased with increasing punch velocity. In addition, α-lactose monohydrate was more affected by punch velocity than β-lactose anhydrate. On the other hand, the specific permeability P_a of β-lactose anhydrate was smaller than that of α-lactose monohydrate, and the radial tensile strength of β-lactose anhydrate was greater than that of α-lactose monohydrate due to the larger contact area between particles, as shown in Fig. 15(c). Stress relaxation of α-lactose monohydrate was smaller than that of β-lactose anhydrate as particles of the former have difficulty in moving and therefore showed better compress-

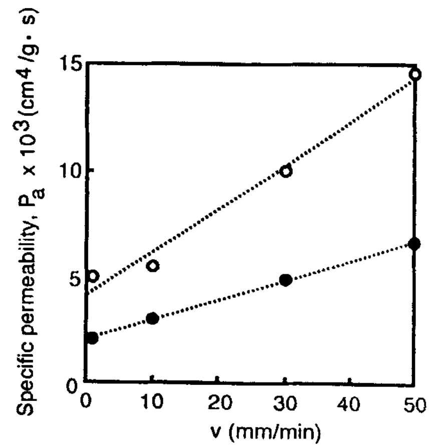

Figure 16. Relationship between punch velocity and specific permeability. ○, α-lactose monohydrate; ●, β-lactose anhydrate.

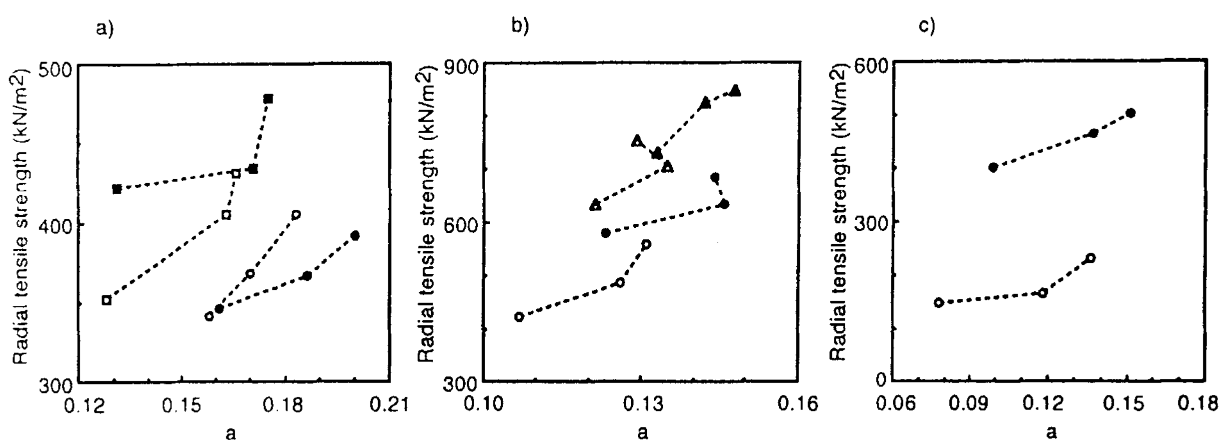

Figure 15. Relationship between constant *a* and radial tensile strength. (a) HPC system; ○, 5% EF-P; ●, 7% EF-P; □, 5% LF-P; ■, 7% LF-P. (b) PVP system; ○, 5% K-30; ●, 7% K-30; Δ, 5% K-90; ▲, 7% K-90. (c) Powder particles; ○, α-lactose monohydrate; ●, β-lactose anhydrate.

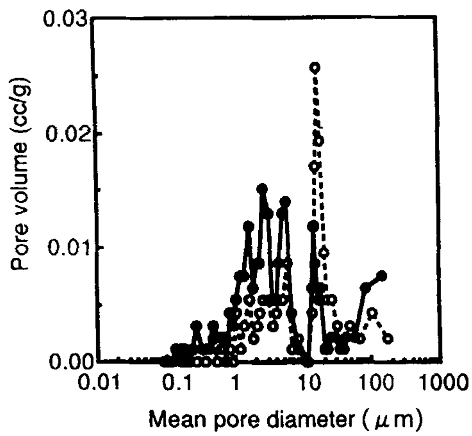

Figure 17. Relationship between mean pore diameter and pore volume. ○, α-lactose monohydrate; ●, β-lactose anhydrate.

ibility than β-lactose anhydrate. However, specific permeability P_a, as determined by the air permeation method, was low for β-lactose anhydrate, which has a more closed structure in tablet form than α-lactose monohydrate.

To investigate these contradictory results, we measured the pore volume distribution in the tablets used by mercury porosimetry. β-Lactose anhydrate has much smaller pore volume than α-lactose monohydrate as shown in Fig. 17. Thus, β-lactose anhydrate particles would form a closer structure in tablets due to their small pores which could not be measured by the air permeation method.

REFERENCES

1. R. J. Roberts and R. C. Rowe, J. Pharm. Pharmacol., 37, 377 (1985); ibid, 39, 70p (1987).
2. K. G. Pitt and J. M. Newton, J. Pharm. Pharmacol., 39, 65p (1987).
3. J. A. Sietz and G. M. Flessland, J. Pharm. Sci., 54, 1353 (1965).
4. J. T. Fell and J. M. Newton, J. Pharm. Sci., 60, 1866 (1971).
5. S. T. David and L. L. Augsburger, J. Pharm. Sci., 66, 155 (1977).
6. N. A. Armstrong, Int. J. Pharm., 49, 1 (1989).
7. P. V. Marshal, P. York, and J. Q. Maclaine, Powder Technol., 74, 171 (1993).
8. Y. Hiramatsu, Y. Seki, and H. Motoyama, Nippon Kogyo Kaishi, 81, 1024 (1965).
9. K. Danjo, K. Kozaki, H. Sunada, and A. Otsuka, Chem. Pharm. Bull., 42, 2121 (1994).
10. K. Danjo, H. Kato, A. Otsuka, and K. Ushimaru, Chem. Pharm. Bull., 42, 2598 (1994).
11. P. York, J. Pharm. Pharmacol., 30, 6 (1978).
12. S. Baba and N. Nagafuji, Shionogi Kenkyu Nempo, 15, 147 (1965).
13. T. Anmo, M. Naritomi, K. Ono, and M. Asano, Yakugaku Zasshi, 89, 359 (1969).
14. Y. Sagawa, T. Sakamoto, and H. Maekawa, Yakuzaigaku, 36, 135 (1976).
15. S. Shlanta and G. Miloslvich, J. Pharm. Sci., 53, 1562 (1964).
16. M. Peleg and R. Moreyra, Powder Technol., 23, 277 (1979).